Supporting Information:

Tunable out-of-plane excitons in 2D single crystal perovskites

Antonio Fieramosca,[†,‡] Luisa De Marco,[*,†] Marco Passoni,[¶] Laura Polimeno,[†,‡] Aurora Rizzo,[†] Barbara L. T. Rosa,[§] Giuseppe Cruciani,[‖] Lorenzo Dominici,[†] Milena De Giorgi,[†] Giuseppe Gigli,[†,‡] Lucio C. Andreani,[¶,⊥] Dario Gerace,[*,¶,†] Dario Ballarini,[*,†] and Daniele Sanvitto[†,#]

† *CNR NANOTEC Institute of Nanotechnology, via Monteroni, 73100, Lecce, Italy*

‡ *Dipartimento di Matematica e Fisica, Università del Salento, Via Arnesano, 73100 Lecce, Italy*

¶ *Dipartimento di Fisica, Università degli Studi di Pavia, Via Bassi 6, 27100 Pavia, Italy*

§ *Universidade Federal de Minas Gerais, Avenida Presidente Antonio Carlos, 6627 - 31270901, Belo Horizonte, Brazil*

‖ *Department of Physics and Earth Sciences, University of Ferrara, Via G. Saragat 1, I-44122 Ferrara, Italy*

⊥ *CNR IFN Istituto di fotonica e nanotecnologie, Piazza L. da Vinci 32, 20133 Milano, Italy*

\# *INFN Istituto Nazionale di Fisica Nucleare, Sezione di Lecce, 73100 Lecce, Italy*

E-mail: luisa.demarco@nanotec.cnr.it; dario.gerace@unipv.it; dario.ballarini@nanotec.cnr.it

Number of Pages: 16

Number of Figures: 11

Number of Tables: 2

Experimental details

Chemicals and Reagents

Phenethylammonium iodide and butylammonium iodide were purchased from Greatcell Solar. Octylamine, hydriodic acid (HI), dichloromethane, ethanol and diethyl ether were purchased from Sigma Aldrich. Lead(II) iodide (PbI_2) was purchased from Alfa Aesar. Gammabutyrolactone was purchased from TCI. All chemicals were used as received without any further purification. SPV 224PR-M adhesive tape was kindly provided by Nitto Denko Corporation.

Synthesis of 2D perovskite flakes

Synthesis of Octylammonium Salt: 20 mL ethanol and 782 mg octylamine were added to a round-bottom flask to form a mixture which was kept at $0°C$ using an ice bath. Then, a stoichiometric amount of HI (2.7 mL of concentrated 57 aqueous HI) was added dropwise. The mixture was stirred for 2.5 h to ensure fully reaction. The solvent was removed by rotary evaporator at $60°C$ and the ammonium salt powder was collected and washed with diethyl ether for three times. Then the powder was dried at $60°C$ under vacuum for 24 h.

PEAI: 498 mg phenethylammonium iodide and 461 mg PbI_2 were dissolved in 1 mL gammabutyrolactone and stirred at $70°C$ for 1 hour. BAI: 403 mg phenethylammonium iodide and 461 mg PbI_2 were dissolved in 1 mL gammabutyrolactone and stirred at $70°C$ for 1 hour. OCT: 514 mg phenethylammonium iodide and 461 mg PbI_2 were dissolved in 1 mL gammabutyrolactone and stirred at $70°C$ for 1 hour.

2D perovskite single crystals were synthesized by Anti-solvent Vapor assisted Crystallization method as follows: 200 micron thick glasses were used as substrates. They were cleaned

with acetone and water in ultrasonic bath for 10 min each and then soaked into a TL1 washing solution ($H_2O_2/NH_3/H_2O$ 5:1:1, v/v), heated at $80°C$ for 10 min to remove organic contamination and finally rinsed 10 times in water. 5 microliters of the perovskite solution are deposited on one of the substrate and immediately after capped by the second glass substrate. Then, a small vial containing 2 mL of dichloromethane is placed on the top of the two sandwiched substrates. Substrates and vial are placed in a bigger Teflon vial, closed with screw cap and left undisturbed for some hours. After this time millimetre-sized crystals appear in between the two substrates having a thickness varying from few to ten micrometres. In this approach, the perovskite precursors solution is exposed to a solvent in which the product is sparingly soluble (thus called anti-solvent); in this way supersaturation is easily reached and precipitation occurs since the solubility of 2D perovskites is drastically reduced. Single crystals are mechanically exfoliated with SPV 224PR-M Nitto Tape and transferred onto glass substrates. The exfoliated flakes, having the thickness of tens of nanometres, appear smooth and uniform over tens of square micrometers, as observed by scanning electron microscopy (SEM) and atomic force microscopy (AFM), see Fig. S2. Samples for SEM and AFM were exfoliated in the same manner and transferred onto Si substrate.

Structural and morphological characterization

X-ray diffraction measurements were performed on single crystals of PEAI, BAI, and OCT 2D-perovskites picked from the glass slide. The smaller and larger dimensions of crystals were ranging from 7 to 15 um and from 65 to 73 um, respectively. Intensity data were collected using an automatic four-circle Nonius KappaCCD diffractometer equipped with a CCD detector (radiation MoKalpha). The software DENZO-SMN was used for refinement of the unit cell and data reduction.

The SEM imaging was performed by the MERLIN Zeiss SEM field emission gun (FEG) instrument at an accelerating voltage of 5 kV using a secondary electron detector.

AFM imaging was carried out using a Park Scanning Probe Microscope (PSIA) in non contact mode. The image acquisition was performed in air at room temperature.

Optical measurements

A home built microscope, equipped with two objectives for reflection and transmission measurements, is used to perform all optical measurements (see Fig.1c of Ref.[S1]). Photoluminescence (PL) is excited through a 10X objective (Rolyn-Rau, N.A.=0.3) and the PL signal is collected by A 60X oil immersion microscope objective (Olympus, N.A.=1.49). The detected signal is focused, by using a 50cm lens, into a 300mm spectrometer (Princeton Instruments, Acton Spectra Pro SP-2300) coupled to a charge coupled device (Princeton Instruments, Pixies 400). The spectrometer is equipped with two gratings, 300 g/mm and 1200 g/mm, both of them blazed at 500nm. The 300g/mm grating is used for reflectivity and PL measurements (overall spectral resolution of 2nm). A 20cm lens is additionally used to image the objectives back focal plane (BFP) onto the entrance slits of the spectrometer. Energy vs in-plane momentum reflectivity measurements (Fig.2, Fig.S6 and Fig.S7a) are performed by using a Xenon light source (Korea Spectral Products-ASB-XE-175) that resonantly excites the Fabry-Perot modes through the oil immersion objective. A half-wave plate (AHWP10M-600) and a linear polarizer (LPVISSE100) are placed in front of the spectrometer in order to resolve the two polarizations TE and TM. Propagation and polarization measurements (Fig.4) are performed by using a 640nm CW laser diode (Coherent-BioRay). For PL measurements, a 488nm CW laser (Spectra-Physics) is used to excite the material (Fig.3, Fig.S4, Fig.S5 and Fig.S7a) through a 10X objective. A 500nm cut-off filter (Thorlabs-FEL0500) along the detection line cuts the residual excitation laser intensity. For resonant propagation reported in Fig. S8, a 50 fs pulsed laser (Coherent, TOPAS-Prime 10Kz) is used to resonantly excite the Fabry-Perot modes.

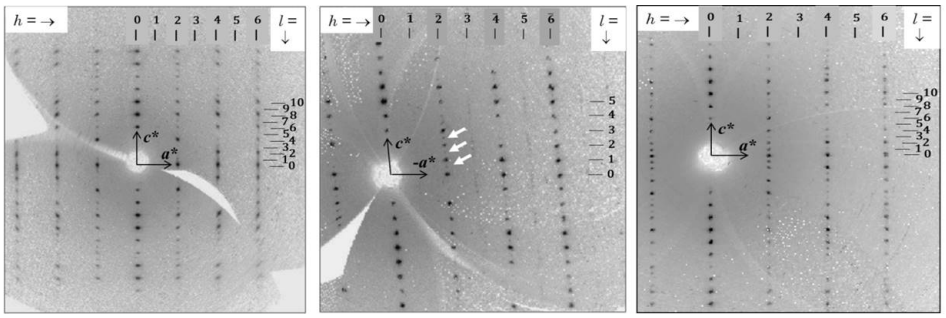

Figure S1: Precession images of the (a*-c*) 0-layer reciprocal plane for 2D-perovskites BAI (left), PEAI (middle), and OCT (right) as reconstructed from measured bidimensional single crystal X-ray diffraction frames. White arrows in PEAI mark the weak diffraction spots revealing a doubling of lattice periodicity along [001] (i.e. about 32.8 instead of 16.4).

Table S1: Summary unit cell parameters and crystal symmetry determined by single crystal XRD for $(BAI)_2PbI_4$, $(PEAI)_2PbI_4$ and $(OCT)_2PbI_4$; the thickness of the inorganic layers are determined by considering the Pb-I apical bond lengths while the thickness of the organic layer is given by the interlayer distance (calculated from the lattice parameters c) subtracted of the inorganic layer height.

	BAI $(C_4H_9NH_3)_2PbI_4$	**PEAI** $(C_6H_5CH_2CH_2NH_3)_2PbI_4$	**OCT** $(C_8H_{17}NH_3)_2PbI_4$
Crystal system:	Orthorhombic	Triclinic	Orthorhombic
Space group:	*P c a b*	*P* $\bar{1}$	*P c a b*
Z:	4	2	4
Lattice parameters:	a = 8.739 Å, b = 8.882 Å, c = 27.772 Å, α = 90.0°, β = 90.0°, γ = 90.0°	a = 8.734 Å, b = 8.747 Å, c = 16.682 Å, α = 95.19°, β = 99.79°, γ = 90.34°	a = 8.691 Å, b = 8.953 Å, c = 37.536 Å, α = 90.0°, β = 90.0°, γ = 90.0°
Unit cell volume:	2155.63 Å^3	1250.47 Å^3	2920.70 Å^3
Inorganic layer thickness	0.638 nm	0.644 nm	0. 638 nm
Organic layer thickness	0.751 nm	1.024 nm	1.239 nm

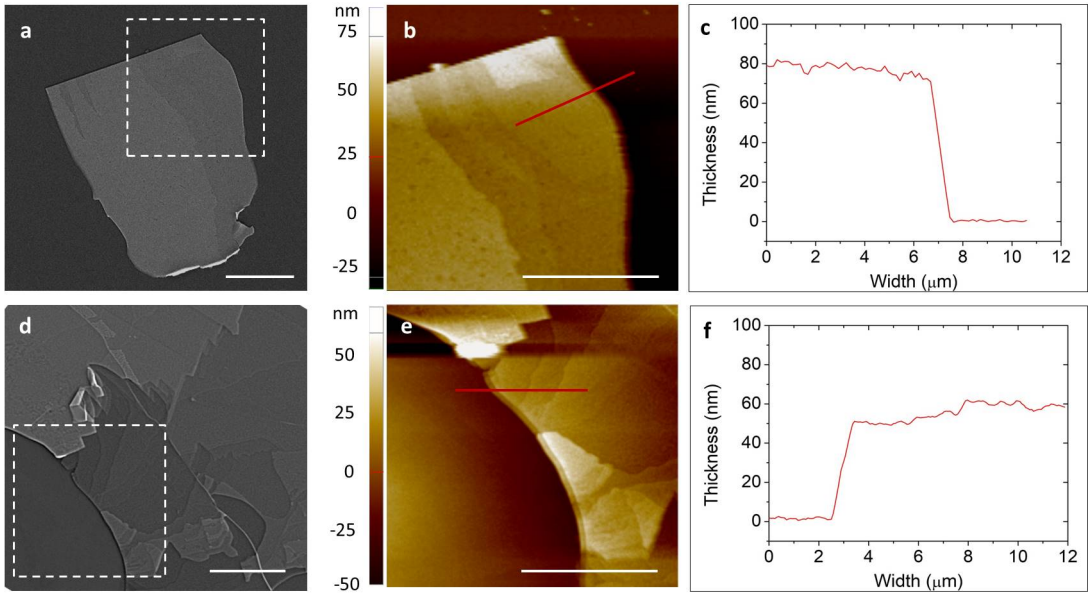

Figure S2: SEM images for $(BAI)_2PbI_4$ (a) and $(OCT)_2PbI_4$ (d) exfoliated crystals. AFM topography images of $(BAI)_2PbI_4$ (b) and $(OCT)_2PbI_4$ (e) in the white square indicated in (a) and (d), respectively. The corresponding height profiles are shown in (c) and (f). SEM scale bars: 20 micron; AFM scale bars: 10 micron

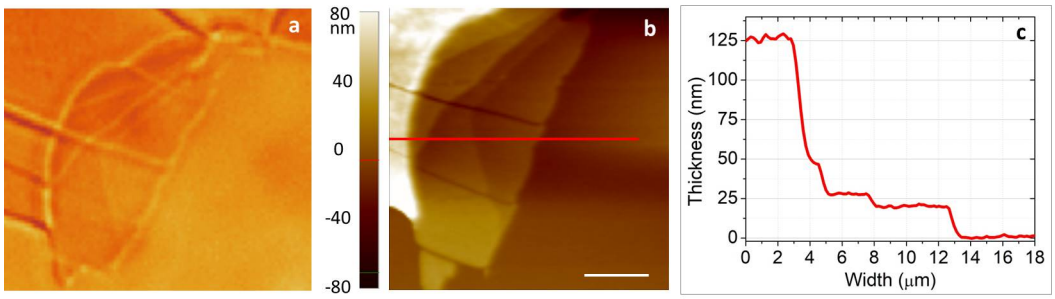

Figure S3: a)Optical image of a PEAI single crystal taken in transmission mode; b) AFM topografy of the same crystal and c) corresponding height profile; AFM scale bar: 5 um.

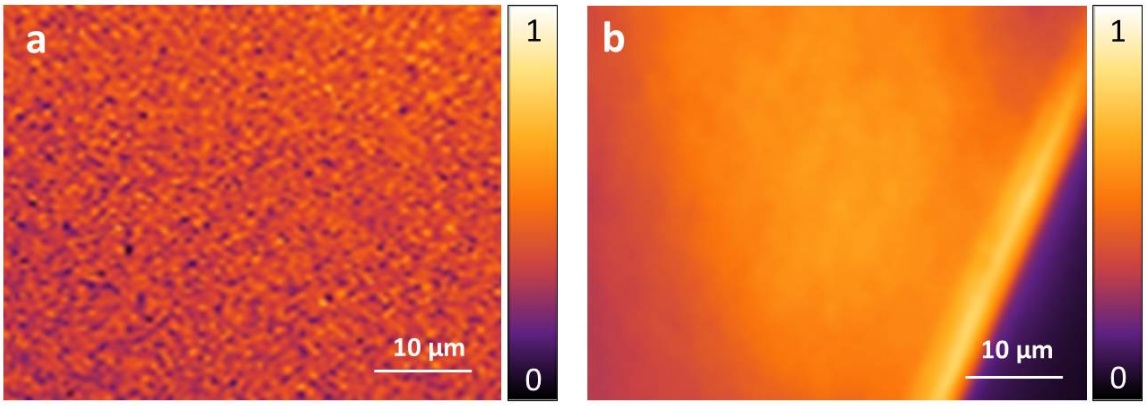

Figure S4: PL image of PEAI polycrystalline film (a) and PEAI single crystal flake (b).

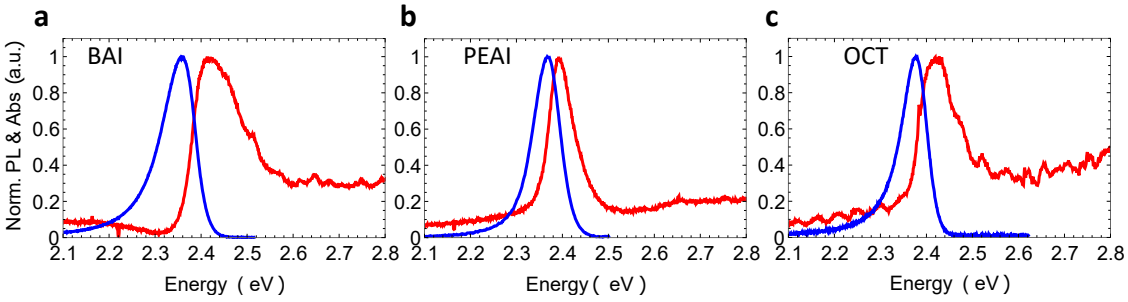

Figure S5: Absorption (Red line) and emission (Blue line) spectra for, respectively, BAI (a), PEAI (b) and OCT (c). A Xenon light source is used to measure the absorption while a CW laser (488nm) is used for PL measurements. The signal from the central part of the flake is considered.

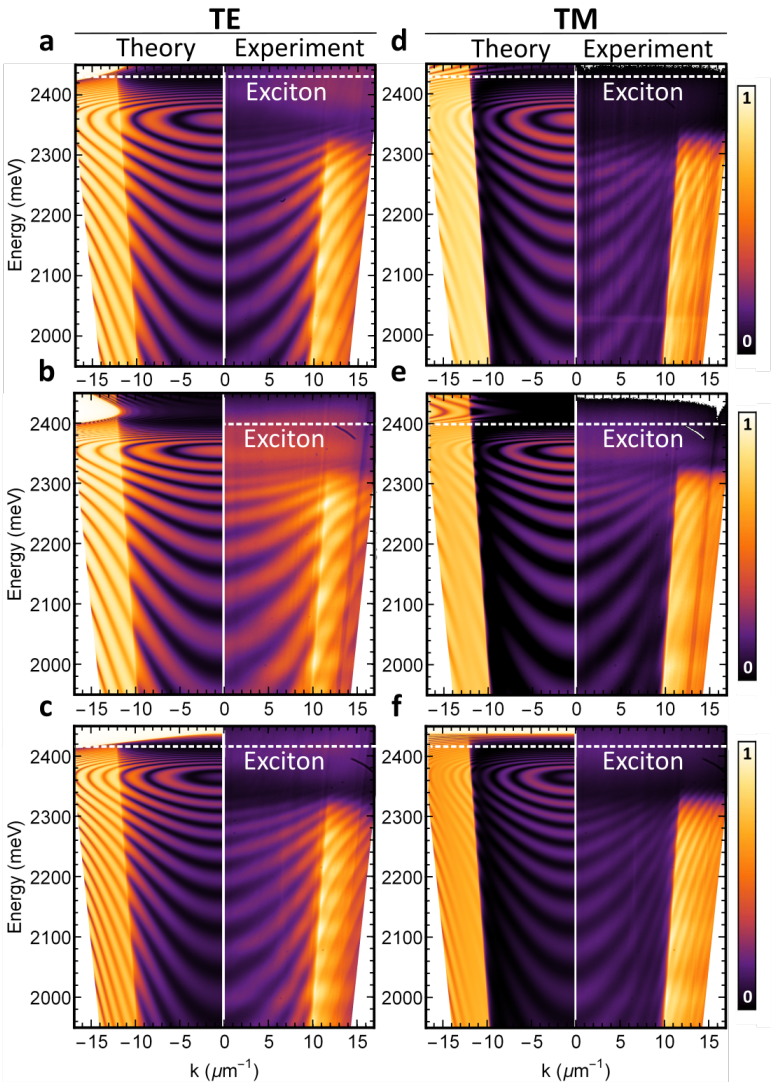

Figure S6: a), b), c) Energy-resolved reflection maps plotted as energy vs in-plane momentum k, measured (right) and calculated (left) for TE polarization for BAI, PEAI and OCT, respectively; d), e), f) Energy-resolved reflection maps, measured (right) and calculated (left) for TM polarization for BAI, PEAI and OCT, respectively.

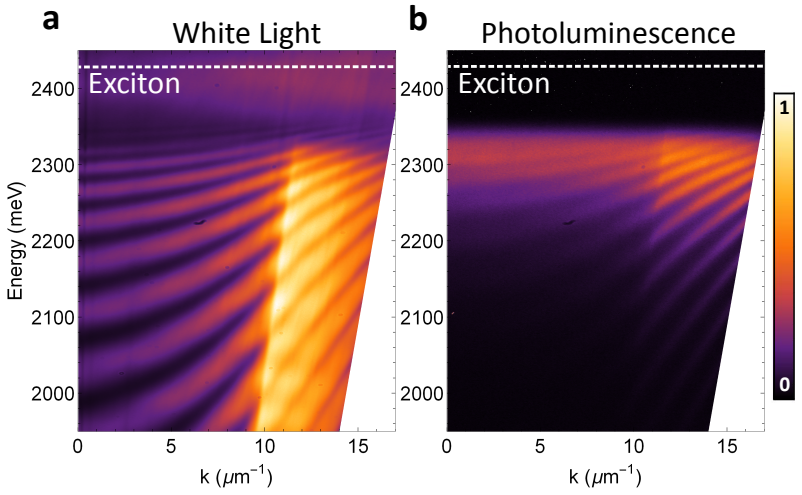

Figure S7: Energy vs in-plane momentum in a) reflection and b) emission configuration for TE polarization, taken in the same spatial position, for BAI crystal 2 um thick. Fabry-Perot resonances appear as dark minimum in reflection (a) and as bright maximum in PL (b).

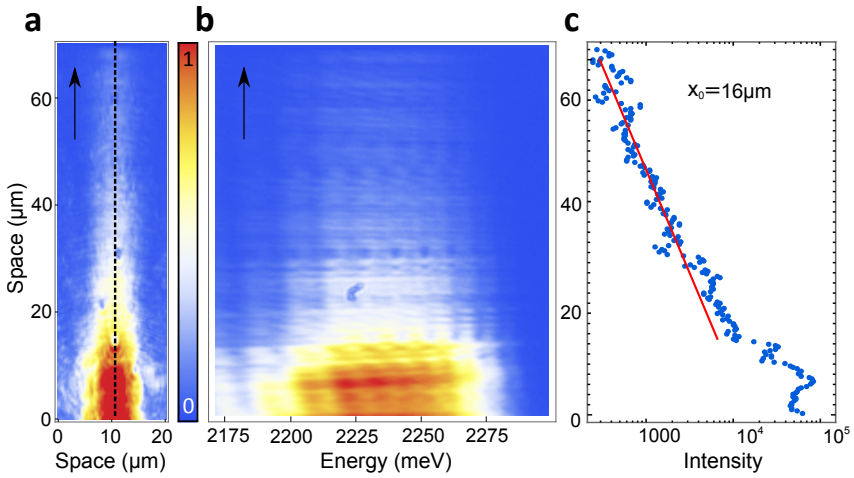

Figure S8: a) Real space propagation for a PEAI crystal of 6um obtained in a resonant configuration with a fs pulsed laser. The laser resonantly excites the Fabry-Prot modes. b) Energy-resolved propagation map (along the black line in S8a); it's possible to recognize the excited propagating modes outside the excitation spot. c) Intensity profile and propagation constant value, exctracted at 2230meV; the value is around 16um and is almost the same for each propagating energy.

The scattering matrix method

General method

The optical response, namely transmission and reflection coefficients, of the perovskite layered crystals is modeled through the Scattering Matrix Method (SMM), as reported in Refs..[S2–S4] In particular, we have implemented a Python version of the method as first devised by Lifeng Li.[S5] We hereby present a short summary of this formulation by using the same notation as in the original reference.[S5] We also introduce a straightforward generalization of the method that allows to model anisotropic materials whose principal axis is along the frame of reference, i.e. described by a diagonal dielectric tensor generically expressed as

$$\varepsilon = \begin{pmatrix} \varepsilon_x & 0 & 0 \\ 0 & \varepsilon_y & 0 \\ 0 & 0 & \varepsilon_z \end{pmatrix} . \tag{1}$$

With reference to the original notation in,[S5] the only modification needed when assuming a rectangular lattice ($\zeta = 0$) is to take the right dielectric tensor element, which is essential to calculate the matrices composing the eigenvalue problem that has to be solved to get the propagation modes inside the single layer. In particular, the matrix $[\![\varepsilon]\!]$ is calculated with the ε_z element, the matrix $\lfloor\lceil\varepsilon\rceil\rfloor$ is calculated with ε_x, and $\lceil\lfloor\varepsilon\rfloor\rceil$ with ε_y, respectively. All the remaining parts of the code, from creation of interface and propagation scattering matrices to the recursion algorithm, are exactly implemented as in the original reference work. Applying the SMM to the present situation, a further simplifying assumption can be made since the structures to be modeled are homogeneous in the xy plane (the perovskite layers are not patterned). Hence, the code can actually be run by only retaining one term in the Fourier expansion of the modes, and actually working with 4×4 scattering matrices. However, we stress that the SMM presented here is general and could be applied to patterned structures.

Simulation details

The structure under study is presented in Fig. S9. Glass and air are assumed as dispersionless and isotropic media with refractive indices 1.49 and 1, respectively. The light is assumed coming from the underside of the structure, with and angle of incidence θ with respect to the normal direction. The plane of incidence is assumed to be the yz plane, so we will speak of TE or s-polarized light when the electric field is along the x direction, and of TM or p-polarized light when the electric field is in the yz plane.

In fact, the interest and originality of the present work mostly lies in the synthesis and optical characterization of layered perovskite crystalline materials, composed by a periodic repetition of thin optically active layers with interposed organic barriers. In this respect, the system is very similar to a multi-quantum well structure typically grown with semiconductor materials. At difference with ordinary quantum well structures, though, these artificial perovskites exhibit strong anisotropic behavior, in addition to an absorption peak due to excitonic-like response. We may assume that the excitonic states are confined in the inorganic layers.

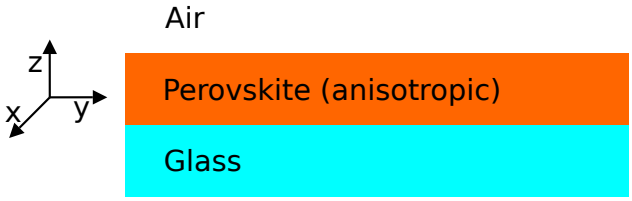

Figure S9: Schematic setup of the simulation and the related reference frame.

As a consequence, we modeled these perovskites as thin layers of anisotropic materials possessing both in-plane and out-of-plane components, namely with a dielectric tensor generically expressed as

$$\varepsilon = \begin{pmatrix} \varepsilon_{\parallel} & 0 & 0 \\ 0 & \varepsilon_{\parallel} & 0 \\ 0 & 0 & \varepsilon_{\perp} \end{pmatrix} . \tag{2}$$

To account for the anisotropic excitonic-like behavior, we assumed dispersive Lorentz ex-

pressions for both $\varepsilon_{\parallel}$ and $\varepsilon_{\perp}$, superimposed to a Cauchy background, i.e.

$$\varepsilon(E) = \varepsilon_c(E) + \varepsilon_l(E)\,, \tag{3}$$

where

$$\varepsilon_c(E) = \left(n_b + AE^2\right)^2 \tag{4}$$

is the general expression for the Cauchy contribution, in which n_b and A are parameters extracted from ellipsometry measurements in the region outside the excitonic absorption, while the Lorentz term is assumed in the usual semiconductor-like form[S6]

$$\varepsilon_l(E) = \frac{E_{\mathrm{LT}}}{E_0 - E - i\Gamma} \tag{5}$$

in which E_0 and Γ are the resonance energy and broadening (full width at half maximum), respectively, as extracted from the ellipsometry measurements in the region corresponding to the excitonic absorption peak. In the Lorentz expression, $E_{\mathrm{LT}} = \hbar^2 e^2 f_{\mathrm{osc}}/(2\varepsilon_0 m_0 E_0 d)$, in which ε_0 (vacuum dielectric permittivity), e (electric charge) and m_0 (rest electron mass) are fundamental constants, while f_{osc} is the oscillator strength associated to the excitonic transition for a perovskite layer thickness d. Since in the spectral region of interest is difficult to distinguish between in-plane and out-of-plane contributions to n_b directly from ellipsometry measurements, we assumed the value extracted in the absorptive region as a mean value, and E_0 and Γ are taken to the same values for both components of the dielectric tensor. The values assumed for each of the crystalline compounds analyzed in this work are explicitly reported in table S2. We notice that the oscillator strength is the main quantity to be adjusted and extracted through our SMM simulations by comparison with experimental reflectivity spectra, assuming different values for in and out-of plane components, respectively. We remind that all energies are expressed in eV in our numerical simulations, which are used to calculate reflectivity spectra for both TE and TM polarized input radiation, respectively.

The spectra thus obtained are directly compared to the experimental ones, which allows to get a reliable quantitative estimate for the in and out-of plane values of the oscillator strengths. The results of such an analysis are reported in the main text.

Table S2: Table with the data extracted from ellipsometry measurements for the three material synthesized and characterized in this work.

	In-plane Cauchy		Out-of-plane Cauchy		Lorentz	
Material	n_b	A	n_b	A	E_0	Γ
BAI	1.628	0.04278	1.789	0.04386	2.41	0.0524
PEAI	1.765	0.04484	1.855	0.04484	2.39	0.0334
OCT	1.490	0.02179	1.692	0.02179	2.41	0.0448

For the comparison between resonant and non-resonant effective medium, as shown in panel 2c of the main text, we employed the indices reported in the figure S10.

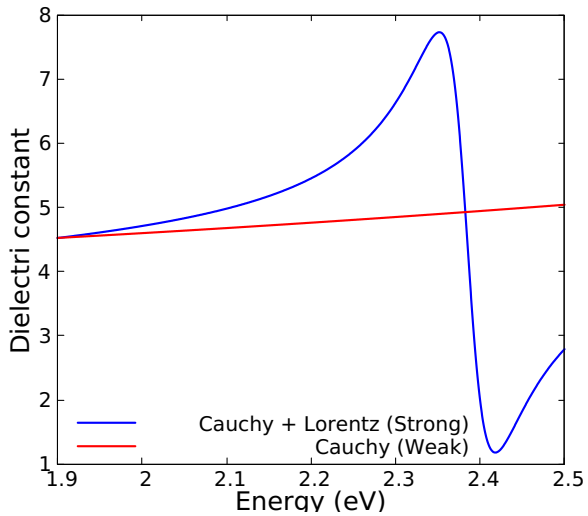

Figure S10: **Cauchy index of the perovskite layer.**

Ordinary and extraordinary refractive index

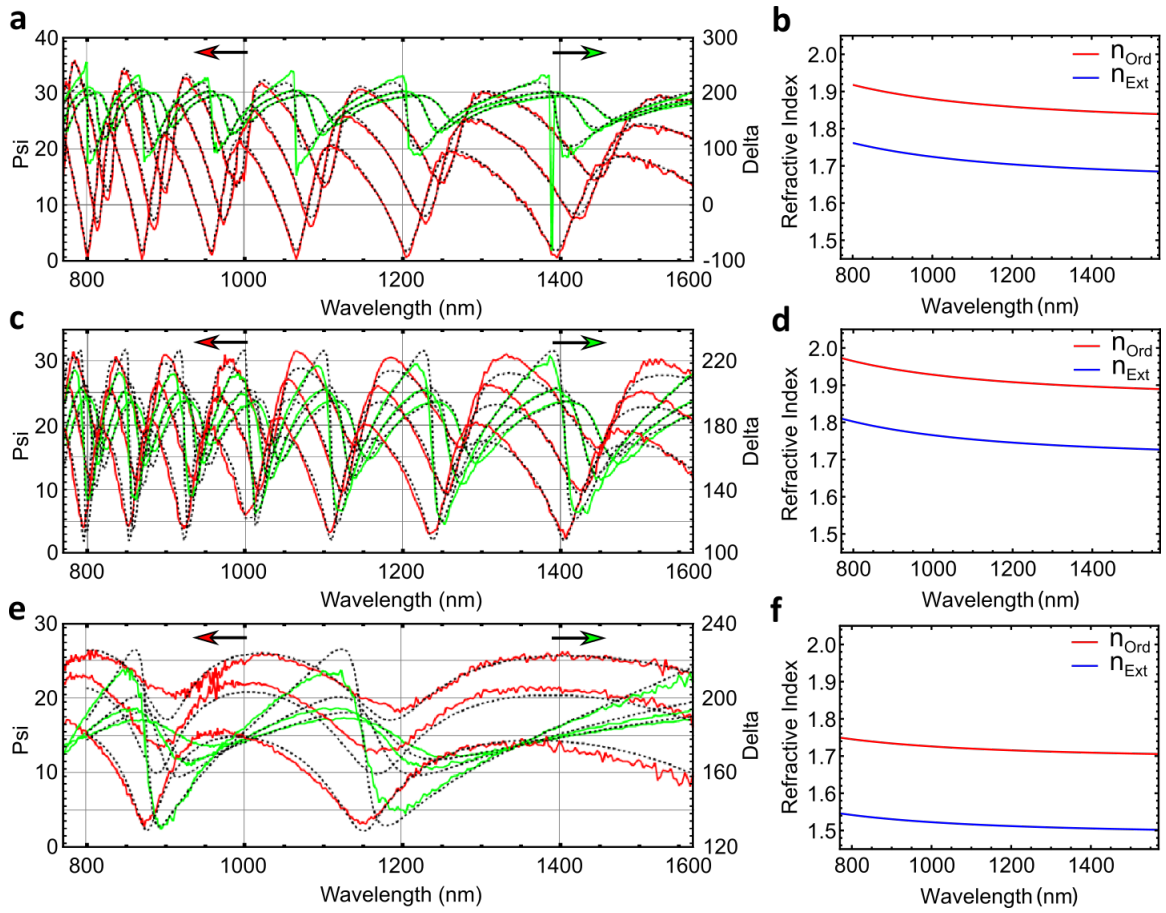

Figure S11: Fitting ellipsometric measurements in the transparent region of BAI (a), PEAI (c) and OCT (e). The corresponding ordinary and extra-ordinary refractive index are shown in b), d) and e) for BAI, PEAI and OCT, respectively.

The real part of the extraordinary n_{ext} and of the ordinary n_{ord} refractive indexes have been evaluated by ellipsometric measurements (J.A. Wollam-EC-400). The single crystal perovskite is deposited on a glass substrate and the thickness is measured by a profilometer. In order to collect signal from the central part of the flake a lens system is used to reduce the spot size. A scan over the angle of incidence is performed in the region around the Brewster angle. The experimental results for Ψ and Δ are reported in the left part of Fig. S11, together with the model, for three different incident angles (40°, 50°, 55°). The asymmetric oscillations in the transparent region suggest an optical anisotropy that is evident for each

kind of material. We used a Cauchy model obtaining good fitting for the three materials, with the corresponding results for n_{ext} and n_{ord} reported in the right panel of Fig. S11.

References

(S1) G. Lerario, D. Ballarini, A. Fieramosca, A. Cannavale, A. Genco, F. Mangione, S. Gambino, L. Dominici, M. De Giorgi, G. Gigli, D. Sanvitto, "High-speed flow of interacting organic polaritons," *Light: Science and Application*, **2017**, *6*, e16212 .

(S2) L. Li, "Formulation and comparison of two recursive matrix algorithms for modeling layered diffraction gratings," *J. Opt. Soc. Am. A* **1996**, *13*, 1024.

(S3) D. M. Whittaker and I. S. Culshaw, "Scattering-matrix treatment of patterned multilayer photonic structures," *Phys. Rev. B* **1999**, *60*, 2610.

(S4) M. Liscidini, D. Gerace, L. C. Andreani, and J. Sipe, "Scattering-matrix analysis of periodically patterned multilayers with asymmetric unit cells and birefringent media," *Phys. Rev. B* **2008**, *77*, 035324.

(S5) L. Li, "New formulation of the Fourier modal method for crossed surface relief gratings," *J. Opt. Soc. Am. A* **1997**, *14*, 2758.

(S6) L. C. Andreani, "Exciton-polaritons in superlattices," *Phys. Lett. A* **1994**, *192*, 99.